Contribution from the Department of Chemistry,
Indian Institute of Technology, Madras 600 036, India

Exchange Interactions in Bis(tetramethylammonium) Bis(maleonitriledithiolato)cuprate(II), $[NMe_4]_2[Cu(mnt)_2]$: A Quasi-1-D Weak-Exchange System

P. KUPPUSAMY and P. T. MANOHARAN*

Received August 29, 1984

The title compound crystallizes with a columnar packing of $Cu(mnt)_2^{2-}$ ions, which are unusually nonplanar. Angular-, frequency-, and temperature-dependent EPR line widths and line positions have been studied in detail to estimate the intra- as well as the interstack exchange interactions. The intrastack (isotropic) exchange (J) has been found to be temperature dependent, and it increases from 600 ± 100 G at 300 K to 1050 ± 100 G at 10 K. However, the interstack exchange (J' = 36 ± 7 G) does not vary with temperature. The ratio $J'/J = 6 \times 10^{-2}$ at 300 K is low enough to make the interactions one-dimensional but at the same time sufficient enough to give rise to Lorentzian line shapes.

Introduction

The presence of columnar crystallographic packing in low-dimensional magnetic materials results in highly anisotropic magnetic, electrical, and optical properties. For example, exchange coupling between electrons in a low-dimensional paramagnetic solid is stronger along the chain when compared to that between the chains. An important quantity in the understanding of the spin dynamics in these quasi-1-D systems is the degree of one-dimensionality, i.e., the ratio of the interchain to intrachain exchange, J'/J. EPR in systems with strong exchange, in general, leads to an exchange-narrowed line whose shape, angular, frequency, and temperature dependence, etc. yields information about the dimensionality of the exchange-coupled network and about the local magnetic interactions.[1-3] In many respects the EPR technique is superior to other methods, such as magnetic susceptibility measurements; for example, even such small interchain effects can be very precisely estimated. Though J' can also be determined from neutron scattering experiments,[4] the energy resolution is generally not sufficient to measure the small dispersion perpendicular to the chain.

Hughes et al.[5] have estimated the intersite exchange coupling J' in $CuCl_2(py)_2$ (py = pyridine) using the frequency-dependent line width of the single line arising as a result of averaging of the two lines corresponding to the two inequivalent sites in the crystal. Even if the chains are not inequivalent, a rough estimation of J' can be made by studying the Fourier components of the spin correlation functions as has been done by Huang and Soos.[6] This paper describes our studies on the exchange interactions (intrachain as well as interchain) present in the quasi-1-D weak-exchange system bis(tetramethylammonium) bis(maleonitriledithiolato)cuprate (II), $[NMe_4]_2[Cu(mnt)_2]$.

Experimental Section

$[NMe_4]_2[Cu(mnt)_2]$ was prepared according to the reported procedures.[7,8] Well-formed black crystals were grown from 1:1 aqueous methanol solutions.

EPR measurements were made with a Varian E-4 spectrometer at X-band and with a Varian E-112 spectrometer at Q-band frequencies. DPPH was used as a g calibrant. The error in g values is ±0.002. The low-temperature measurements were done in a JEOL X-band instrument using an Air Products liquid-helium cryostat.

The morphology of the crystal used for EPR measurements is shown in Figure 1. Measurements were made with the magnetic field in the ab, bc, and ac^* planes. The error in the peak-to-peak line width (ΔB_{pp}) is ±2 G.

Results and Discussion

Crystal Structure. $[NMe_4]_2[Cu(mnt)_2]$ belongs to the monoclinic crystal system with space group $P2_1/c$. The unit cell parameters are

$$a = 12.230\ (3)\ \text{Å} \qquad b = 11.518\ (9)\ \text{Å} \qquad c = 16.269\ (6)\ \text{Å}$$
$$\beta = 95.07\ (2)^\circ$$

Of the four molecules per unit cell, two are magnetically inequivalent and are related by a 2-fold rotation about the b axis. The other two are related to the first two by an inversion symmetry and hence are magnetically equivalent to their inversion counterparts. The crystal structure[9] consists of $Cu(mnt)_2^{2-}$ planes stacked in columns along the a axis of the unit cell. Along the stack direction the copper atoms are not collinear, show slight alternation (7.811 and 7.841 Å), and follow these sequences: x, y, z; $\bar{x}$, $\bar{y}$, $\bar{z}$; $1 + x$, y, z; $1 + \bar{x}$, $\bar{y}$, $\bar{z}$; and so on. The shortest interchain (inequivalent) Cu–Cu distance is 8.288 Å. The normal to the least-squares $Cu(mnt)_2^{2-}$ plane makes an angle of 28.1° with the stack axis.

The projections of the structure onto ab and bc planes, based on coordinates from ref 9, are shown in Figures 2 and 3, respectively. The anion in the present system has a nonplanar geometry, which is quite unusual. The nonplanarity has been attributed to the presence of several short contact distances between the atoms of the anion and the cations of the monoclinic lattice. In $[MB]_2[Cu(mnt)_2]\cdot(CH_3)_2CO$ (MB = methylene blue cation) also a similar nonplanarity has been reported.[10]

Electron Paramagnetic Resonance. Some preliminary EPR work on this system has been reported by Standley and Taylor.[11] They doped $Cu(mnt)_2^{2-}$ into the nickel analogue $[NMe_4]_2[Ni(mnt)_2]$ for which the structure had been known[12] already as triclinic with a planar NiS_4 core. The reported spin Hamiltonian parameters are

$$g_\parallel = 2.090 \pm 0.005 \qquad A_\parallel = \pm(162 \pm 3) \times 10^{-4}\ \text{cm}^{-1}$$
$$g_\perp = 2.017 \pm 0.002 \qquad A_\perp = \pm(42 \pm 2) \times 10^{-4}\ \text{cm}^{-1}$$

These authors have mentioned that mixed crystals of $[NMe_4]_2[Cu(mnt)_2]$ diluted in $[NMe_4]_2[Ni(mnt)_2]$ grown from solutions containing 25% by weight of copper salt were triclinic. This along with the fact that pure copper salt is monoclinic and has a nonplanar metal chelate unit suggests that the $Cu(mnt)_2^{2-}$ ion in the nickel lattice is planar. Further evidence for the planarity is

(1) Richards, P. M. "Low Dimensional Cooperative Phenomena"; Keller, H. J., Ed.; Plenum Press: New York, 1975.
(2) Soos, Z. G.; Huang, T. Z.; Valentine, J.; Hughes, R. C. *Phys. Rev. B: Solid State* **1973**, *8*, 993.
(3) Hone, D. W.; Richards, P. M. *Annu. Rev. Mater. Sci.* **1974**, *4*, 337.
(4) Skalyo, J., Jr.; Shirane, G.; Friedberg, S. A.; Kobayashi, H. *Phys. Rev. B: Solid State* **1970**, *2*, 4632.
(5) Hughes, R. C.; Morosin, B.; Richards, P. M.; Duffy, W., Jr., *Phys. Rev. B: Solid State* **1975**, *11*, 1795.
(6) Huang, T. Z.; Soos, Z. G. *Phys. Rev. B: Solid State* **1974**, *9*, 4981.
(7) Davison, A.; Holm, R. H. *Inorg. Synth.* **1971**, *10*, 8.
(8) Billig, E.; Williams, R.; Bernal, I.; Waters, J. H.; Gray, H. B. *Inorg. Chem.* **1964**, *3*, 663.
(9) Mahadevan, C.; Seshasayee, M. *J. Crystallogr. Spectrosc. Res.* **1984**, *14*, 213.
(10) Snaathorst, D.; Doesburg. H. M.; Perenboom, J. A. A. J.; Keijzers, C. P. *Inorg. Chem.* **1981**, *20*, 2526.
(11) Standley, K. J.; Taylor, P. F. *J. Phys. C* **1968**, *1*, 551.
(12) Maki, A. H.; Edelstein, N.; Davison, A.; Holm, R. H. *J. Am. Chem. Soc.* **1964**, *86*, 4580.

0020-1669/85/1324-3053$01.50/0

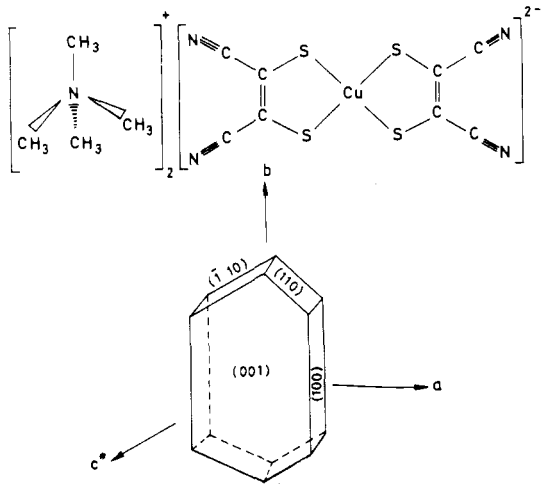

Figure 1. Structural formula and morphology of $[NMe_4]_2[Cu(mnt)_2]$.

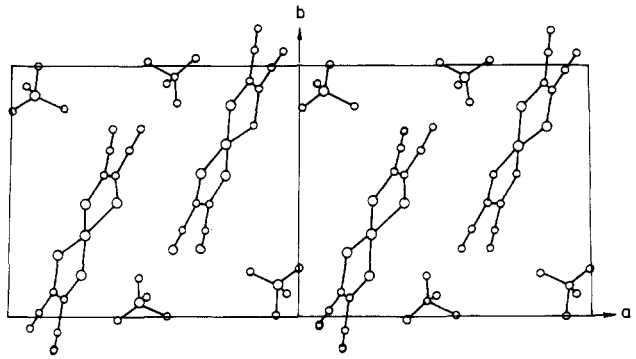

Figure 2. Projection of the structure onto the *ab* plane.

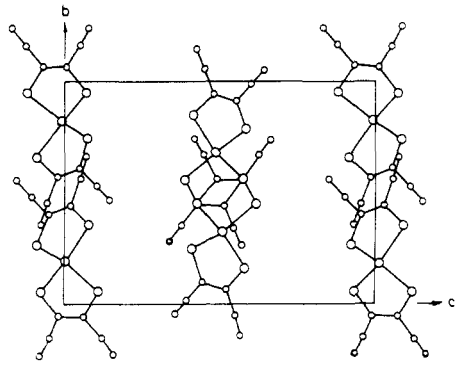

Figure 3. Projection of the structure onto the *bc* plane.

obtained from the fact that the hyperfine tensors closely resemble those reported[12] for the planar $Cu(mnt)_2^{2-}$ system. Had it been nonplanar, at least the hyperfine tensor would be significantly different.[10] Hence, it is obvious that the nonplanarity is present only in the pure salt. This feature combined with the observation that the stacking of the anions along the chain shows slight alternation prompted us to investigate the nature of the interactions present in this system by detailed EPR measurements. The EPR results are presented and discussed below under separate headings.

(i) g Tensor. EPR measurements were made with the magnetic field vector scanning the three orthogonal planes *ab*, *bc*, and *ac** at both X- and Q-band frequencies. At X-band only a single line was observed at all orientations, indicating that the exchange between the two magnetically inequivalent sites is stronger than half the separation between them, i.e., $J' > (\Delta g \beta B)/2$. However, at Q-band in the *ab* plane two resonances could be seen, well-resolved for most of the orientations, with maximum separation between the two lines being 340 G when $\vec{B}$ is 40° away from the *a* axis. The separation of the sites in the *bc* plane is even smaller at Q-band with the result that only one line is seen at the average of the two resonance fields. A simple diagonalization procedure yielded the principal values of the averaged **g** tensor (X-band) to be

$$g_1 = 2.024 \pm 0.002 \qquad g_2 = 2.034 \pm 0.002$$
$$g_3 = 2.076 \pm 0.002$$

These values are significantly different from the molecular g values, which are reported to be $g_x = 2.023$, $g_y = 2.026$, and $g_z = 2.086$.[12]

The $\mathbf{g}_{mol}$ of the two chains, e.g. A and B, are equivalent except for their different orientations. The Hamiltonian is

$$\mathcal{H} = \mathcal{H}_Z^A + \mathcal{H}_Z^B + \mathcal{H}_{ex}^O + \mathcal{H}_{ex}^{AB}$$
$$= \beta\vec{B}\cdot\mathbf{g}_A\cdot\vec{S}_A + \beta\vec{B}\cdot\mathbf{g}_B\cdot\vec{S}_B - 2J\,\vec{S}_A\cdot\vec{S}_{A+1} - 2J_{AB}\,\vec{S}_A\cdot\vec{S}_B \quad (1)$$

where J is the isotropic exchange between spins A and A + 1 along the chain A (which is equivalent to that in chain B). J_{AB} is the exchange coupling between the two spins on chains A and B. The first two Zeeman terms can be written as

$$\mathcal{H}_Z = \mathcal{H}_Z^O + \mathcal{H}_Z' \quad (2)$$

with

$$\mathcal{H}_Z^O = \beta\vec{B}\cdot\mathbf{g}\cdot\vec{S} \quad (3)$$
$$\mathcal{H}_Z' = \beta\vec{B}\cdot\Delta\mathbf{g}\cdot\vec{s} \quad (4)$$

where

$$\vec{S} = \vec{S}_A + \vec{S}_B \quad (5)$$
$$\vec{s} = \vec{S}_A - \vec{S}_B \quad (6)$$
$$\mathbf{g} = \tfrac{1}{2}(\mathbf{g}_A + \mathbf{g}_B) \quad (7)$$

and

$$\Delta\mathbf{g} = \tfrac{1}{2}(\mathbf{g}_A - \mathbf{g}_B) \quad (8)$$

Now it is possible to get the exchange-averaged **g** tensor by assuming the molecular **g** tensor and the direction cosines for the two inequivalent sites and averaging them in the reference coordinate system.[13] If, for example, $\bar{\bar{C}}$ is the rotation matrix consisting of the direction cosines of the three principal axes X, Y, and Z of one of the two inequivalent sites with respect to the crystal axes a, b, and c^*, then the rotation matrix of the other site, which is related to the first one by a 2-fold rotation, is given by $\bar{\bar{C}}\cdot\bar{\bar{D}}$, where

$$\bar{\bar{D}} = \begin{pmatrix} -1 & 0 & 0 \\ 0 & 1 & 0 \\ 0 & 0 & -1 \end{pmatrix} \quad (9)$$

The corresponding two **g** tensors in the orthogonal reference system, $\mathbf{g}^1_{cryst}$ and $\mathbf{g}^2_{cryst}$, are related to the molecular **g** tensor, $\mathbf{g}_{mol}$, by

$$\mathbf{g}^1_{cryst} = \bar{\bar{C}}^{-1}\cdot\mathbf{g}_{mol}\cdot\bar{\bar{C}} \quad (10)$$
$$\mathbf{g}^2_{cryst} = \bar{\bar{D}}\bar{\bar{C}}^{-1}\cdot\mathbf{g}_{mol}\cdot\bar{\bar{C}}^{-1}\bar{\bar{D}} \quad (11)$$

The above expressions lead to

$$(g^1_{cryst})_{ij} = (g^2_{cryst})_{ij}$$

if $i + j$ is even and

$$(g^1_{cryst})_{ij} = -(g^2_{cryst})_{ij}$$

if $i + j$ is odd. The average **g** tensor is equal to the arithmatic average of $\mathbf{g}^1_{cryst}$ and $\mathbf{g}^2_{cryst}$ and so is given by

$$\mathbf{g} = \mathbf{g}^{av}_{cryst} = \begin{pmatrix} (g^1cryst)_{11} & 0 & (g^1cryst)_{13} \\ 0 & (g^1cryst)_{22} & 0 \\ (g^1cryst)_{31} & 0 & (g^1cryst)_{33} \end{pmatrix} \quad (12)$$

Also we obtain

$$\Delta\mathbf{g} = \mathbf{g}_A - \mathbf{g}_B = \begin{pmatrix} 0 & (g^1cryst)_{12} & 0 \\ (g^1cryst)_{21} & 0 & (g^1cryst)_{23} \\ 0 & (g^1cryst)_{32} & 0 \end{pmatrix} \quad (13)$$

(13) Mooij, J. J.; Klaassen, A. A. K.; de Boer, E. *Mol. Phys.* **1976**, *32*, 879.

Table I. Experimental and Calculated Principal Values of g and Their Direction Cosines

g values	direction cosines		
	a	b	c^*
Molecular Values			
$g_x = 2.021$	0.257	0.772	0.581
$g_y = 2.025$	−0.395	−0.465	0.792
$g_z = 2.088$	0.882	−0.433	0.186
Average Values (Experimental X-Band)			
$g_1 = 2.024$	−0.190	−0.042	0.981
$g_2 = 2.033$	0.034	0.998	0.049
$g_3 = 2.077$	0.981	−0.043	0.189
Average Values (Calculated)			
$g_1 = 2.024$	−0.196	0	0.981
$g_2 = 2.034$	0	1	0
$g_3 = 2.076$	0.981	0	0.196

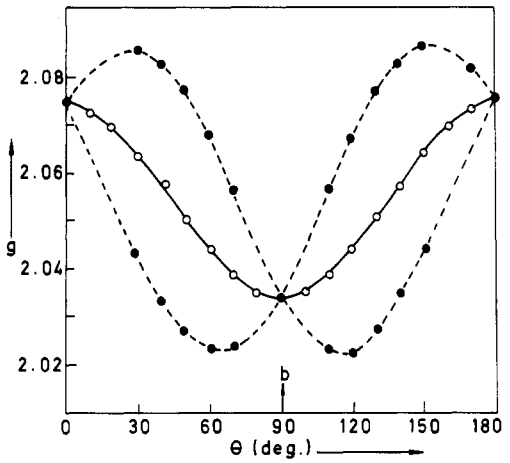

Figure 4. Experimental and calculated angular variations of g in the ab plane; (---) simulation for individual sites; (●) experimental points at Q-band; (—) simulation after averaging; (○) experimental points at X-band.

The Δg term gives rise to nonsecular broadening, which is negligible as long as $\omega_0 t_c >> 1$, where ω_0 is the Zeeman frequency and t_c is the correlation time for the interchain spin diffusion.[14] From the expression (12) it is evident that one of the principal axes lies along the b axis while the other two are somewhere in the ac^* plane. The other two principal values and their direction cosines can be obtained by diagonalizing the **g**-tensor matrix.

In the present system there is an uncertainty in the choice of the molecular **g** tensor as well as its direction cosines, owing to the nonplanarity of the $Cu(mnt)_2$ unit. The presence of nonplanarity does not seem to affect the molecular g values much. For instance, Snaathorst et al.[10] have reported $g_\parallel = 2.090$ and $g_\perp = 2.024$ for the nonplanar system $[MB]_2[Cu(mnt)_2]\cdot(CH_3)_2CO$ while the normal values[12] are $g_1 = 2.023$, $g_2 = 2.026$, and g_3 ($\equiv g_\parallel$) = 2.086. However, it appears that the hyperfine coupling tensor is very sensitive to distortions. In $[MB]_2[Cu(mnt)_2]\cdot(CH_3)_2CO$ the A values are 10% smaller than those reported for planar systems. The twisting of the ligands in the present nonplanar system can be better viewed as a mutual rotation of the two chelate planes in the opposite directions with respect to the 2-fold axis bisecting the chelate C=C bond for ±20.57° such that the normals to the chelate planes make an angle of 41.14°. Such a twisting should then leave the **g**-tensor directions with respect to the reference axes unaltered. The g_z direction is chosen along the normal to the least-squares plane containing the whole anion while g_x is along the 2-fold axis of the chelate lying in the least-squares plane and passing through the midpoint of the C=C bond. The calculated and observed (after averaging) direction cosines match very well (see Table I).

With use of the calculated direction cosines and with $g_x = 2.021$, $g_y = 2.025$, and $g_z = 2.088$ the exchange-averaged **g** tensor was obtained by the procedure described above. The agreement between the calculated and observed g values (X-band) is excellent as is seen in Figure 4. In Figure 5 is shown the matching of the observed and the simulated g values in the ac^* plane where the two sites are equivalent.

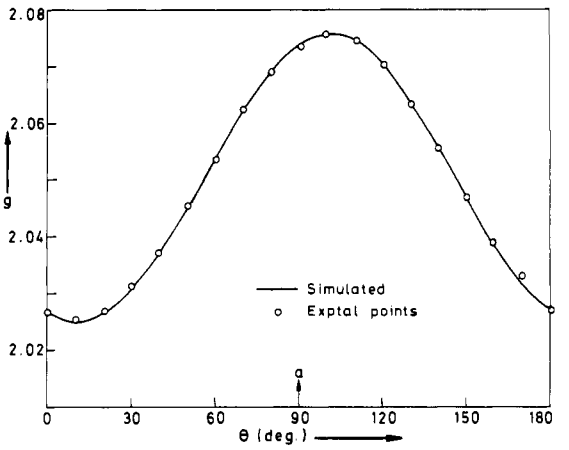

Figure 5. Angular variation of g in the ac^* plane: (—) simulated and (○) experimental points.

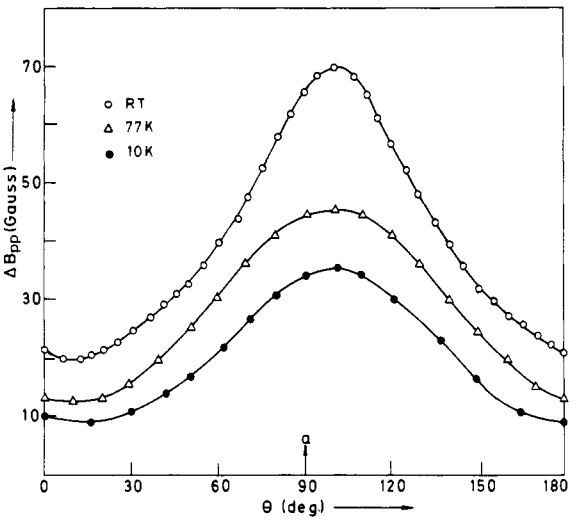

Figure 6. Angular variation of line width in the ac^* plane at X-band at 300, 77, and 10 K.

(ii) Line Width and Line Shape. The angular variation of line width in the ac^* plane, where the chains are magnetically equivalent, is shown in Figure 6. It is evident that the dominating interaction that is contributing to the line width anisotropy is hyperfine whose principal axes coincide with that of the **g** tensor. In this plane no significant difference in line width was observed between X- and Q-band measurements. This might happen when the exchange interaction J is far off from X- and Q-band frequencies, i.e.

$$\mathcal{H}_{ex} >> \mathcal{H}_Q > \mathcal{H}_X$$

or

$$\mathcal{H}_{ex} << \mathcal{H}_X < \mathcal{H}_Q$$

In the former case both secular and nonsecular components of the hyperfine and dipolar fields will be contributing fully to the observed line width while in the latter case only secular components will be effective in broadening the observed line. In the intermediate case, with

$$\mathcal{H}_X < \mathcal{H}_{ex} < \mathcal{H}_Q$$

one would observe frequency-dependent line widths as the nonsecular contributions to the Q-band line widths are only partial.

Magnetic susceptibility measurements down to 4.2 K did not show any magnetic ordering. Further, the variation of susceptibility with temperature was found to be in accordance with the

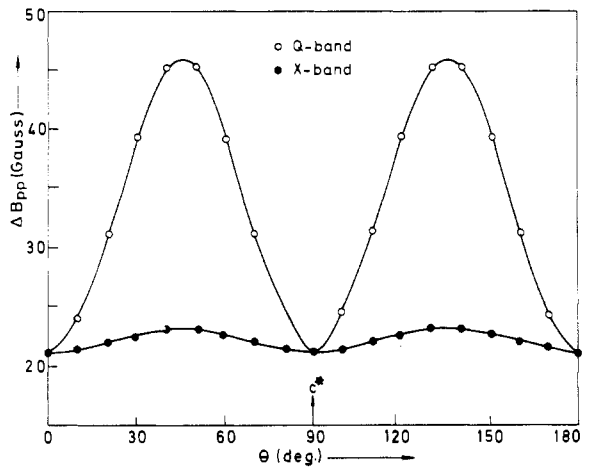

Figure 7. Angular variation of line width in the *bc* plane at X- and Q-band frequencies.

Curie–Weiss law with negligible Weis correction.

The line shape analysis in the *ac** plane showed the shape of the resonance to be close to Lorentzian at all angles, indicating that (i) the interactions are not purely 1-D and (ii) the exchange interaction is sufficiently stronger than the broadening mechanisms such as hyperfine or dipolar.

On the other hand, the *bc* plane line widths were observed to be frequency dependent. The X- and Q-band line widths at room temperature are shown in Figure 7. The Q-band line widths are larger than the X-band line widths except when $\vec{B}||b$ or c^* axis. In this plane there must be two resonances corresponding to the two inequivalent sites, and since the intersite exchange frequency is larger compared to the separation between them even at Q-band there is an incomplete averaging with the width of the resulting line varying as roughly (splitting)^2/(exchange rate). Hence a comparison of the line widths at these two Zeeman frequencies is used to make an estimate of the intersite exchange J'. This is discussed in detail later in this paper.

(iii) Intrastack Exchange, J. The line width information available in the *ac** plane was used to get an estimate of the intrastack (isotropic) exchange parameter J. Though the two sites are equivalent in the *ac** plane, the effective field due to the $\Delta\mathbf{g}$ term in eq 13 does not vanish and is given by [14]

$$\vec{B}_e = \vec{B}\cdot\Delta\mathbf{g} \tag{14}$$

The effective field B_e is seen perpendicular to the *ac** plane where the axis of quantization defined by $\vec{B}\cdot\mathbf{g}$ lies and will give rise to nonsecular broadening effects. The above effect is shown[15] to be negligible when $\omega_0 t_c >> 1$. In our case $t_c = 6 \times 10^{-10}$ s (vide supra) and hence $\omega_0 t = 5.7$ at X-band and 21.0 at Q-band. Therefore, this contribution to line width can be neglected.

In the strong exchange narrowing case the line width ΔB_{pp} is given by [16]

$$(3^{1/2}/2)\Delta B_{pp} = \frac{M_2^{t}}{J} \tag{15}$$

where M_2^t is the sum of dipolar and hyperfine second moments. The full second moment is used when $J >> \hbar\omega_0$, where ω_0 is the Zeeman frequency. When $J << \hbar\omega_0$ only the secular ($\Delta m = 0$) part of the second moment will be effective in contributing to the observed line width. In the intermediate case one will observe frequency-dependent nonsecular contribution and hence line width. In the present case, as no frequency-dependent line width (in the *ac** plane) is observed, we are certainly not in the intermediate region.

The dipolar and hyperfine second moments were calculated as described elsewhere.[2,17] The variation of the secular part of the second moments is shown in Figure 8. As M_2^t(secular) follows the observed line width variation in this plane, we have used only the secular part of the second moments. This is also justified by the successful analysis of the data.

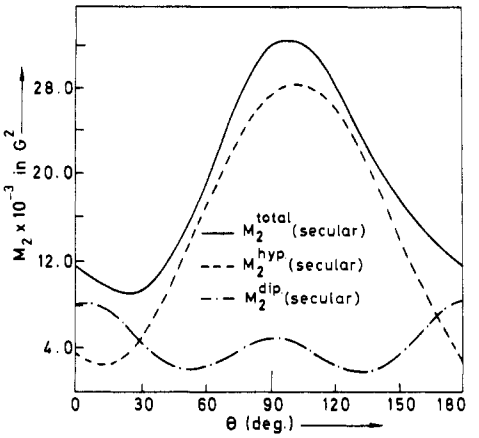

Figure 8. Angular variation of local fields in the *ac** plane.

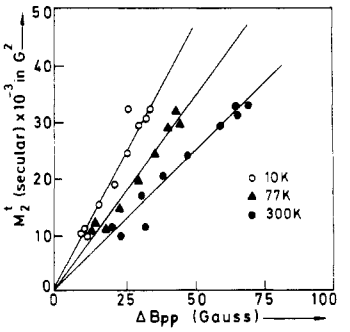

Figure 9. Correspondence between M_2^t(secular) and ΔB_{pp}(experimental) in the *ac** plane at 300, 77, and 10 K (cf. eq 15).

Though the data at one orientation is sufficient to estimate J using eq 15, we find from Figure 9 that there is good agreement between the two quantities over the entire set of data in this plane. The fitting gives a value of 600 ± 100 G for J for the room-temperature data in the *ac** plane.

(iv) Interstack Exchange, J'. The line width data at X- and Q-band frequencies in the *bc* plane were used to estimate the effective intersite exchange field, H_e, as well as J'. For $J' > (\Delta g)\beta B/2$, we would observe a single line and the theories of exchange averaging[14] predict that the width of the line varies as the square of the splitting ΔB (in gauss) of the sites

$$\Delta B_{pp} = (\Delta B)^2/H_e \tag{16}$$

where H_e is defined as the effective intersite exchange field. If the measurements are done at two different frequencies, e.g. X- and Q-band, then

$$\Delta B_{pp}^{Q} - \Delta B_{pp}^{X} = \frac{(\Delta B_Q)^2 - (\Delta B_X)^2}{H_e} \tag{17}$$

where ΔB_X and ΔB_Q are the differences in the expected resonance fields of the two sites at X- and Q-bands, respectively, in the absence of J'. The quantity H_e depends on the rate of exchange between inequivalent sites and is given by[5]

$$(g\beta/\hbar)H_e = 4t_c^{-1}(3^{1/2}/2) \tag{18}$$

where $t_c^{-1} = 0.16\hbar|J|^{1/3}/|J'|^{4/3}$ is the correlation time for interchain spin diffusions. The angular variation of X- and Q-band line widths in the *bc* plane (Figure 7) can be satisfactorily fit into expression 17 for $H_e = 300 \pm 50$ G. This gives a value of $(6 \pm 1) \times 10^{-10}$ s for t_c.

(14) Yokota, M.; Koide, S. *J. Phys. Soc. Jpn.* **1954**, *9*, 953.
(15) Ramakrishna, B. L.; Manoharan, P. T. *Mol. Phys.* **1984**, *52*, 65.
(16) Van Vleck, J. H. *Phys. Rev.* **1948**, *74*, 1168.
(17) McGregor, K. T.; Soos, Z. G. *J. Chem. Phys.* **1976**, *64*, 2506.

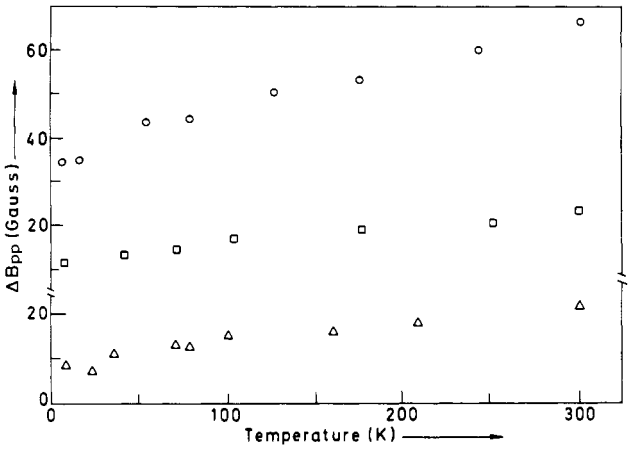

Figure 10. Temperature dependence of line widths at X-band with $\vec{B}\|a$ (○), $\vec{B}\|b$ (□), and $\vec{B}\|c^*$ (△).

Now assuming $J = 600 \pm 100$ G obtained from the line width data in the ac^* plane at room temperature, we obtain $J' = 36 \pm 7$ G. The ratio $J'/J = 6 \times 10^{-2}$ is low enough to make the interactions one-dimensional but at the same time sufficient enough to cut off the long time diffusive behavior of spins in pure 1-D chains giving rise to the observed Lorentzian line shapes.

(v) Temperature Variation. The anisotropic line widths are strongly temperature dependent and decrease smoothly with temperature. The line width measurements were carried out down to 10 K at X-band. The angular variations of the line width in the ac^* plane at 77 and 10 K are found in Figure 6. The line width, for example, when $\vec{B}\|a$ decreases by ~67% at 77 K and by ~50% at 10 K. The temperature-dependent linewidth with magnetic field vector along the three crystallographic reference vectors a, b, and c^* is shown in Figure 10. It should be noted that in all the three orientations the relative decrease in line widths at different temperatures are the same. In other words the rate of variation of line width ΔB_{pp} with temperature is constant regardless of orientation. This may be due to temperature-dependent J or J'.[16] We have further observed that the relative decrease in ΔB_{pp} vs. T is the same in the ab and ac^* planes also. This observation rules out the temperature dependence of J', since it is expected that J' will affect the line widths of the ab and/or bc plane differently from that of the ac^* plane at any Zeeman frequency due to inequivalency of the sites. Hence, it is believed that J' does not increase on cooling.

Using the angular variation of ΔB_{pp} at 77 K and at 10 K, in the ac^* plane we can calculate the J values as described earlier using eq 15. The line width data at 77 K and 10 K fit quite reasonably with J values of 800 ± 100 and 1050 ± 100 G, respectively. These are shown along with the room-tempeature data in Figure 9. We are able to further justify the temperature dependence of J by calculating J for some intermediate temperatures using the widths at $\vec{B}\|c^*$ and $\vec{B}\|a$. All these values of J as a function of temperature are clearly demonstrated in Figure 11. It is true that for intermediate temperatures no full angular variation of ΔB_{pp} has been measured. However, it is gratifying to note that the temperature variation of J has been clearly demonstrated. It is necessary to mention here that an assumption has been made that the calculated dipolar second moments based on room temperature crystal data do not vary much on cooling. This assumption may not be strictly valid because of the possibility of lattice contractions at lower temperatures. It is supposed that in the case of $[NMe_4]_2[Cu(mnt)_2]$ being of hyperfine-dominated line width, no erroneous conclusion can be made by the above assumption.

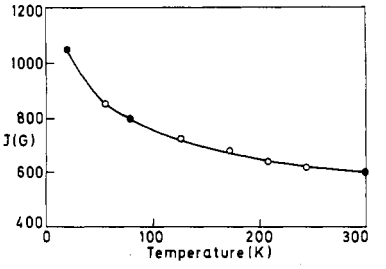

Figure 11. Temperature dependence of J. ● denotes J based on the whole set of data in the ac^* plane at the respective temperatures while ○ denotes J based on $\vec{B}\|c^*$ and $\vec{B}\|a$ data only.

Summary and Conclusions

Quite unusual nonplanar geometry of the complex anion in this lattice is comparable to what has been observed in $[MB]_2[Cu(mnt)_2]$.[10] The nonplanarity combined with the stacking of the anions along the chain with a slight alternation makes it an interesting system for line width studies by EPR. The lattice of $[NMe_4]_2[Cu(mnt)_2]$ represents a quasi-1-D weak-exchange system. Though the inter- and intrastack exchanges are weak with $J = 600 \pm 100$ G and $J' = 36 \pm 7$ G, the ratio of $J'/J = 6 \times 10^{-2}$ is low enough to make the interactions one-dimensional but at the same time sufficient enough to cut off the long time diffusive behavior of spins in pure 1-D chains giving rise to the observed Lorentzian line shapes. The temperature variation of ΔB_{pp}, though indicating an increased J at lower temperatures, does not change its quasi-1-D character considerably.

Acknowledgment. This work was supported by a scheme from the Department of Science and Technology, Government of India, New Delhi, India, for which we are grateful.

Registry No. $[NMe_4]_2[Cu(mnt)_2]$, 20084-76-8.